0026-895X/06/6904-1328–1337$20.00
MOLECULAR PHARMACOLOGY
Copyright © 2006 The American Society for Pharmacology and Experimental Therapeutics
Mol Pharmacol 69:1328–1337, 2006

Vol. 69, No. 4
20701/3094562
Printed in U.S.A.

Bradycardic and Proarrhythmic Properties of Sinus Node Inhibitors

Juliane Stieber, Karen Wieland, Georg Stöckl, Andreas Ludwig, and Franz Hofmann

Institut für Pharmakologie und Toxikologie der Technischen Universität München, München, Germany

Received November 10, 2005; accepted December 30, 2005

ABSTRACT

Sinus node inhibitors reduce the heart rate presumably by blocking the pacemaker current I_f in the cardiac conduction system. This pacemaker current is carried by four hyperpolarization-activated, cyclic nucleotide-gated cation (HCN) channels. We tested the potential subtype-specificity of the sinus node inhibitors cilobradine, ivabradine, and zatebradine using cloned HCN channels. All three substances blocked the slow inward current through human HCN1, HCN2, HCN3, and HCN4 channels. There was no subtype-specificity for the steady-state block, with mean IC_{50} values of 0.99, 2.25, and 1.96 μM for cilobradine, ivabradine, and zatebradine, respectively. Native I_f, recorded from mouse sinoatrial node cells, was slightly more efficiently blocked by cilobradine (IC_{50} value of 0.62 μM) than were the HCN currents. The block of I_f in sinoatrial node cells resulted in slower and dysrhythmic spontaneous action potentials. The in vivo action of these blockers was analyzed using telemetric ECG recordings in mice. Each compound reduced the heart rate dose-dependently from 600 to 200 bpm with ED_{50} values of 1.2, 4.7, and 1.8 mg/kg for cilobradine, ivabradine, and zatebradine, respectively. β-Adrenergic stimulation or forced physical activity only partly reversed this bradycardia. In addition to bradycardia, all three drugs induced increasing arrhythmia at concentrations greater than 5 mg/kg for cilobradine, greater than 10 mg/kg for zatebradine, or greater than 15 mg/kg for ivabradine. This dysrhythmic heart rate is characterized by periodic fluctuations of the duration between the T and P wave, resembling a form of sick sinus syndrome in humans. Hence, all available sinus node inhibitors possess an as-yet-unrecognized proarrhythmic potential.

The hyperpolarization-activated, cyclic nucleotide-gated cation current termed I_h or I_f is a prominent depolarizing current in a variety of neuronal and cardiac cells that show spontaneous electrical activity (Robinson and Siegelbaum, 2003; Baruscotti et al., 2005). In the heart, this current is especially found in the cardiac conduction system [e.g., in Purkinje fibers and sinoatrial node cells (pacemaker cells)], in which it is believed to mediate the β-adrenergic stimulation of the heart rate via its direct modulation by cAMP. Four HCN channels underlie the native I_f with an as-yet-unknown subtype assembly to produce the tissue- and cell-specific I_f throughout the organism. In the sinoatrial node, HCN4 is the predominant subtype in all species, whereas HCN1, HCN2, and HCN3 are expressed at lower levels and with less specificity for the sinoatrial node compared with the myocardium (Marionneau et al., 2005).

The physiological role of I_f in the adult cardiac conduction system, especially the relevance of I_f for heart rate regulation, has not been fully elucidated to date. HCN2 knockout mice show slight sinus arrhythmia at rest, but in these mice, I_f in sinoatrial cells is only reduced, not eliminated (Ludwig et al., 2003). HCN4 knockout mice die during embryonal development (Stieber et al., 2003a). The heart of these embryos is beating but at a slow pace, which can be attributed to missing pacemaker potentials as a result of the almost complete lack of I_f in the developing cardiac cells. However, this does not allow conclusions about the role of I_f/HCN4 in the adult organism. There are no reports about a cardiac phenotype of HCN3 or HCN1 knockout mice.

Sinus node inhibitors (SNIs) have been shown to block the native I_f in cells of the cardiac conduction system and in neurons of various species (Bogaert et al., 1990; BoSmith et al., 1993; Bois et al., 1996), even before HCN channels have been identified as the underlying ion channels (Ludwig et al., 1998; Santoro et al., 1998) and thus as possible targets of sinus node inhibitors. The block of I_f in sheep Purkinje fibers or rabbit sinoatrial node cells results in a slower or, in the case of Purkinje fibers, even abolished spontaneous slow

This work was supported by grants from Deutsche Forschungsgemeinschaft and Fond der Chemie.
Article, publication date, and citation information can be found at http://molpharm.aspetjournals.org.
doi:10.1124/mol.105.020701.

ABBREVIATIONS: HCN, hyperpolarization-activated, cyclic nucleotide-gated cation channel; HEK, human embryonic kidney cells; AP, action potential; SAN, sinoatrial node; SNI, sinus node inhibitor; DDR, diastolic depolarization rate; MDP, maximal diastolic potential; CL, cycle length; CL-SD, standard deviation of the cycle length; AV, atrioventricular.

depolarization. The slowing effect on sinoatrial node depolarization has been assumed consequently to be the reason for the bradycardic action of these substances (DiFrancesco and Camm, 2004). For several years, ivabradine, a member of the newer SNIs which also include cilobradine and zatebradine, has been tested in animals (Vilaine et al., 2003; Colin et al., 2004; Du et al., 2004; Monnet et al., 2004) and humans (Borer et al., 2003). It has been found that although this substance has a depressing effect on the heart rate, neuronal side effects are limited to occasional visual symptoms. This led to the clinical development of SNIs as specific bradycardic agents. In addition, SNIs could serve as a tool to study the effects of I_f inhibition, specifically in the cardiac conduction system in vivo. In this study, we addressed two issues: first, we sought to determine the effects of an increasing inhibition of I_f on the mammalian heart rate regulation; and second, we investigated whether sinus node inhibitors preferably target certain HCN subtypes.

Materials and Methods

Molecular Cloning of Human HCN Channels. Human HCN2 and HCN4 cDNAs were originally cloned from the atrioventricular node region of a human heart (Ludwig et al., 1999), and human HCN1 and HCN3 cDNAs were cloned from Whole Human Brain QUICK-Clone cDNA (Clontech, Mountain View, CA) (Stieber et al., 2005). All cDNAs were subcloned into the pcDNA3 mammalian expression vector (Invitrogen, Karlsruhe, Germany).

Functional Expression of HCN Channels and Electrophysiological Recordings. Expression of HCN channels in HEK293 cells and voltage-clamp experiments were basically done as described previously (Stieber et al., 2003b). In brief, HEK293 cells were transfected with expression vectors encoding one of the human HCN channels using FuGENE6 transfection reagent (Roche, Mannheim, Germany) according to the manufacturer's instructions (transfectant/DNA ratio: 3:1, v/w) or by electroporation using a Bio-Rad system (Bio-Rad, München, Germany) according to the manufacturer's instructions. Cells were cultured on polylysated glass coverslips in a modified Dulbecco's modified Eagle's medium complete medium (Quantum 286; PAA Laboratories, Pasching, Austria) and kept at 37°C in 8.5% CO_2. Currents from transfected cells were recorded with the whole-cell patch-clamp recording technique at a temperature of 23 ± 1°C. Patch pipettes were pulled from borosilicate glass and had a resistance of 2 to 5 MΩ when filled with intracellular solution containing 10 mM NaCl, 30 mM KCl, 90 mM potassium aspartate, 1 mM $MgSO_4$, 5 mM EGTA, and 10 mM HEPES, with pH adjusted to 7.4 with KOH. During the recordings, cells were continuously superfused with extracellular (bath) solution containing 120 mM NaCl, 20 mM KCl, 1 mM $MgCl_2$, 1.8 mM $CaCl_2$, 10 mM HEPES, and 10 mM glucose, with pH adjusted to 7.4 with NaOH. All chemicals for these solutions were obtained from Sigma (Taufkirchen, Germany). Chemical structures of the sinus node inhibitors used are displayed in Fig. 1. Stock solutions (10 mM; in double-distilled H_2O) of cilobradine (Boehringer, Biberach, Germany), ivabradine (Institut de Recherches Servier, Suresnes, France), zatebradine (Boehringer Ingelheim Pharma KG, Biberach, Germany), and verapamil (Tocris, Bristol, UK) were stored as aliquots at −20°C for a maximum of four weeks and were diluted into the extracellular solution to the appropriate concentration on the day of the experiment. Application of the drug to the cells was performed by complete exchange of the bath solution with bath solution containing the indicated drug concentration and continuous superfusing. The membrane potential was held at −40 mV. To elicit inward currents, hyperpolarizing steps to −100 mV were repeatedly applied. The protocol used to obtain use-dependent block was as follows (Fig. 2A): first, there was a drug wash-in period of 10 min; cells were clamped at −40 mV during this time. Then, there was repetition of the following activation/deactivation step: HCN1, −100 mV for 0.5 s/−40 mV for 0.5 s; HCN2, −100 mV for 2 s/−40 mV for 2 s; HCN3, −100 mV for 2 s/−40 mV for 2 s; and HCN4, −100 mV for 10 s/−40 mV for 10 s. The different durations were chosen to account for the different activation/deactivation kinetics of the HCN channels. At the end of the activation pulse, an open probability of 0.5 was reached for each HCN subtype. It is postulated that in this open configuration SNIs are able to bind to the blocking site inside the pore (DiFrancesco and Camm, 2004).

Data were acquired using an Axopatch 200B amplifier and pClamp7 software or a MultiClamp 700A amplifier and pClamp9 software (all from Molecular Devices, Union City, CA). Analysis was done offline with Origin 6.0. (OriginLab Corp., Northampton, MA). HCN current amplitude was defined as the amplitude at the end of the activation pulse minus the amplitude of the initial lag. The first activation after the drug wash-in period was taken as baseline, and the amplitudes of the subsequent activations were used to calculate the percentage of block at each activation relative to the first activation. Maximal achievable block for each drug concentration was reached within 30 min. IC_{50} values were obtained by fitting the logarithmically plotted data (percentage of block) with a sigmoidal fit/logistic model: $y = A_2 + (A_1 - A_2)/(1 + (x/x_0)^p)$, where x_0 corresponds to the IC_{50} value. The Hill coefficient was defined as the slope of this logarithmic fit. Statistical significance was tested by comparing the data sets (percentage of block) for each drug concentration/HCN subtype using the Student's t test. p values < 0.05 were considered significant.

Preparation of Sinoatrial Node Cells from Murine Hearts and Electrophysiological Recordings. Sinoatrial node (SAN) cells for electrophysiological recordings were basically prepared as described previously (Ludwig et al., 2003). In brief, 2- to 3-month-old C57/Bl6 mice were deeply anesthetized with 100 mg/kg ketamine (Ketavet; Pharmacia GmbH, Erlangen, Germany) and 10 mg/kg xylazine (Rompun; Bayer AG, Leverkusen, Germany), injected intraperitoneally. The beating hearts were quickly removed and placed in prewarmed Tyrode's solution containing 140 mM NaCl, 5.4 mM KCl,

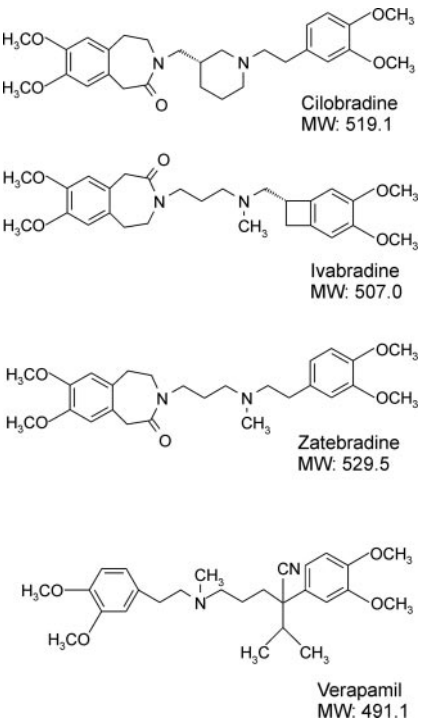

Fig. 1. Chemical structures and molecular weights (MW) of the SNIs cilobradine (DK-AH269), ivabradine (S16257–2), and zatebradine (UL-FS49), and the related calcium-channel blocker verapamil. All substances in this study were used as hydrochloride salts.

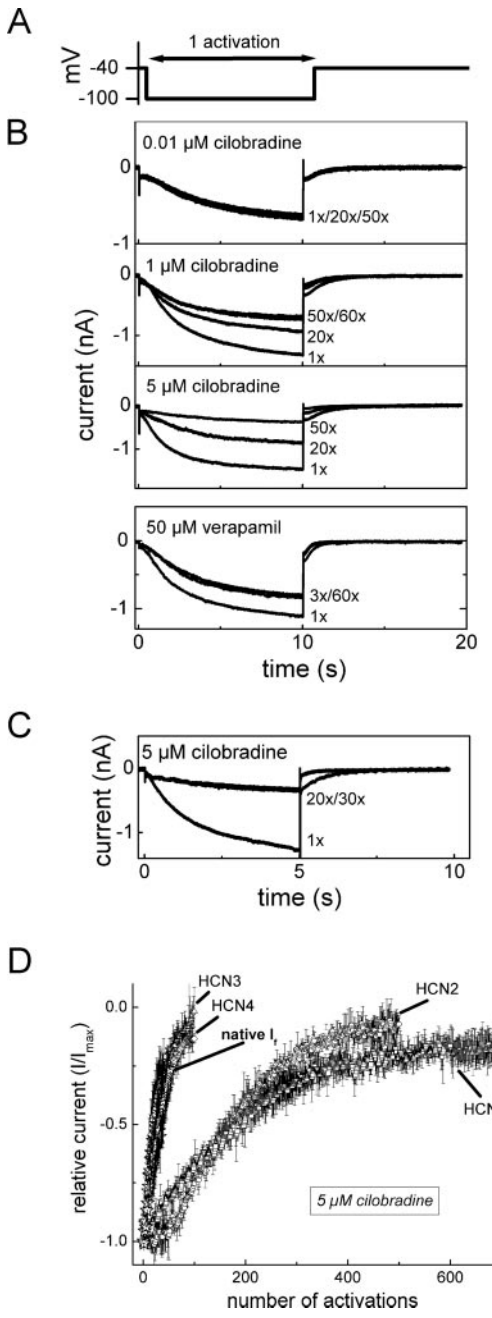

Fig. 2. Use-dependent block of HCN currents and native I_f. A, pulse protocol for the voltage-clamp measurements of HCN channels, expressed in HEK293 cells, and I_f, recorded from isolated mouse sinoatrial node cells. Duration of activation/deactivation depends on HCN subtype as described under *Materials and Methods*. B, example of use-dependent block of cloned HCN channels, shown for HCN4 in the presence of three concentrations of cilobradine. Inward currents were elicited by applying the pulse protocol described in A. Different cells were used for each measurement. "(Number)x" in the graphics refers to the number of activations at which the current trace was elicited after application of the drug. No block was obtained with 0.01 μM cilobradine after 50 activations, whereas with 5 μM cilobradine, maximum block was achieved with less than 50 activations. In comparison, 50 μM verapamil only induced a small, instant block of HCN4 channels. C, block of native I_f by 5 μM cilobradine. Maximum block for this concentration was achieved after 20 activations. D, comparison of use-dependent block of HCN1, HCN2, HCN3, and HCN4 channels and the native I_f by 5 μM cilobradine. All currents are blocked to the same extent, but only 20 to 40 activations are required for HCN3, HCN4, and I_f to reach this block, whereas 300 to 500 activations are required for HCN1 and HCN2. Values are mean ± S.E.M., n = 4 to 9, for each current. Squares, HCN1; circles, HCN2; triangles, HCN3; diamonds, HCN4; stars, I_f.

1.8 mM $CaCl_2$, 1 mM $MgCl_2$, 5 mM HEPES, and 5.5 mM glucose, pH 7.4. The SAN region between the superior vena cava and the right atrium was excised, minced, and placed into modified Tyrode's solution containing 140 mM NaCl, 5.4 mM KCl, 0.2 mM $CaCl_2$, 0.5 mM $MgCl_2$, 1.2 mM KH_2PO_4, 50 mM taurine, 5 mM HEPES, and 5.5 mM glucose, pH 6.9. Enzymatic digestion of the tissue was carried out for 30 min at 35°C with 1.75 mg/ml collagenase B, 0.4 mg/ml elastase (both from Roche, Mannheim, Germany), and 1 mg/ml bovine serum albumin added to the modified Tyrode's solution. After digestion, the modified Tyrode's solution was replaced by storage solution containing 25 mM KCl, 80 mM L-glutamic acid, 20 mM taurine, 10 mM KH_2PO_4, 3 mM $MgCl_2$, 10 mM glucose, 10 mM HEPES, and 0.5 mM EGTA. The pH was adjusted to 7.4 with KOH. Cells were kept at least 3 h at 4°C in storage solution before they were slowly readapted to calcium-containing solutions.

To compare cloned and native channel properties, I_f from SAN cells was recorded in whole-cell mode under the same conditions as described above for HCN currents in HEK293 cells, especially at the same bath temperature of 23 ± 1°C. The extracellular solution was the same as for recordings from HEK293 cells. The pulse length for repeated activation/deactivation of I_f was 5 s/5 s. The intracellular solution for measurements on native cells contained 10 mM NaCl, 130 mM potassium aspartate, 0.04 mM $CaCl_2$, 2 mM Mg-ATP, 6.6 mM creatine phosphate, 0.1 mM sodium GTP, and 10 mM HEPES, pH 7.3. Spontaneous action potentials (APs) from SAN cells were recorded at 32 ± 1°C using the perforated patch technique with 200 μM amphotericin B added to the intracellular solution. Standard AP parameters were calculated as described previously (Mangoni and Nargeot, 2001).

Telemetric ECG Recordings in Mice. All animal experiments were performed according to the Guide for the Care and Use of Laboratory Animals/U.S. National Institutes of Health. Male C57/Bl6 mice were housed in single cages in a 12-h dark-light cycle environment with free access to food and water. Radiotelemetric ECG transmitters (DSI, St. Paul, MN) were implanted into the peritoneal cavity under general anesthesia with isoflurane/O_2. The ECG leads were sutured subcutaneously onto the upper right chest muscle and the upper left abdominal wall muscle. This resulted approximately in the lead II position of the ECG electrodes. The animals were allowed to recover for at least 2 weeks before the experiments. Stock solutions of cilobradine (4.5 mg/ml), ivabradine (4.5 mg/ml), zatebradine (4.5 mg/ml), and verapamil (2 mg/ml) were prepared in sterile 0.9% NaCl (Braun AG, Melsungen, Germany), kept at −20°C, and diluted with 0.9% NaCl to the desired concentrations in a volume of 100 μl on the day of the experiment. Isoproterenol (Sigma, Taufkirchen, Germany) was dissolved in 0.9% NaCl less than 1 h before the injection. Data were acquired using the DSI acquisition system. ECG signals were sampled every minute for 20 s. After 1-h prerun (unless otherwise noted), the mice were injected intraperitoneally with the drug. The ECGs were recorded for 3 to 24 h thereafter. The animals were allowed to recover for at least 48 h between experiments because the effective half-life of the SNIs was up to 12 h compared with the postulated rather short plasma half-life of only 2 h (ivabradine/Procoralan; Dr. R. Derwand, Servier Deutschland GmbH, personal communication). For forced physical activity, animals were trained to run on a custom-made, electrically driven treadmill at a speed of approximately 0.4 m/s and 20% ascending slope.

As appropriate, before and after the injection of the drug, ECG parameters, heart rate, and heart rate variability were analyzed. The definitions of the ECG intervals are the following: R-R, duration from R to R; P-P, duration from P peak to P peak; PQ, end of P to beginning of Q; QT, beginning of Q to end of T, where end of T is the return of any T deviation to the isoelectric line; QTc, heart rate-corrected QT interval using the equation $QT/(\sqrt{R\text{-}R/100})$ (Mitchell et al., 1998); and TP, end of T to beginning of the next ECG complex's P. The heart rate (in beats per minute) was calculated from the R-R duration (in milliseconds) as 60,000/R-R. The standard deviation of

the R-R duration (RR-SD) as a measure of heart rate variability was calculated as the standard deviation of the R-R durations during a 20-s period. ED_{50} values were obtained by fitting the logarithmically plotted data (heart rate versus drug concentration) with a sigmoidal fit/logistic model: $y = A_2 + (A_1 - A_2)/(1 + (x/x_0)^p)$, where x_0 corresponds to ED_{50} value. On the linear scale, R-R values were fitted with an exponential model: $y = A_1 e^{(-x/t_1)}$, RR-SD could be fitted with a sigmoidal (Boltzmann) model: $y = A_1 + (A_2 - A_1)/(1 + 10^{(\log(x_0) - x)p})$.

Results

Efficient Block of All Four HCN Subtypes by SNIs. SNIs are known blockers of I_f. However, because all four subtypes of HCN channels underlie I_f in the heart, we wanted to know whether any of the sinus node inhibitors could be used to discriminate between HCN subtypes. The inward currents through all expressed HCN channels were blocked dose- and use-dependently by SNIs at low micromolar concentrations. For example, 0.01 μM cilobradine did not inhibit current flow through HCN4 channels, whereas 1 and 5 μM led to increasing inhibition (Fig. 2B). The development of the inhibition was rather slow. The channels had to be repeatedly activated before the maximal inhibition for the respective drug concentration could be observed. Verapamil, on the other hand, a known calcium-channel blocker from which the SNIs have been structurally derived, only induced a small, non–use-dependent block of HCN channels at high concentrations (Fig. 2B, bottom). Similar to HCN currents, the native I_f value of murine SAN cells was blocked efficiently by 5 μM cilobradine (Fig. 2C). Again, the block developed rather "slowly", because repeated activations were necessary for the block to occur. Comparison of the use-dependent block for all HCN subtypes and I_f (Fig. 2D) revealed a difference between the HCN subtypes with respect to the onset of the block. HCN1 and HCN2 channels needed 300 to 500 activations before the steady-state inhibition was reached, whereas HCN3, HCN4, and the I_f were maximally inhibited after 20 to 40 activations. However, the steady-state inhibition reached for each concentration, an important measure for the effectiveness in vivo, did not seem to be influenced by this 10-fold difference in use-dependence (Fig. 3). The steady-state dose-response curves for HCN1- to -4 showed no subtype-specificity. However, there are differences in the efficiency of the individual SNIs (Table 1). Cilobradine was the most efficient substance with a mean IC_{50} value of 0.99 μM, followed by zatebradine (1.97 μM) and ivabradine (2.2 μM). The block of native I_f by cilobradine was similarly efficient with an IC_{50} value of 0.62 μM under the same conditions, measured at room temperature (23 ± 1°C). The slope of the dose-response curves was approximately 1 for each substance and channel (Table 1), suggesting one docking site per channel.

Cilobradine Does Not Abolish Spontaneous Action Potentials in Isolated SAN Cells but Changes Their Shape, Frequency, and Variability. To test the effect of SNIs on action potentials, cilobradine as the most effective HCN channel blocker was chosen. Cilobradine (1 μM) had a prominent effect on spontaneous action potentials recorded from isolated murine SAN cells (compare Fig. 4, A and B). The firing frequency was reduced to approximately half, apparently by prolongation of the duration between action potentials. Statistical analysis of the AP parameters indeed revealed a highly significant prolongation of the cycle lengths from 275 ± 18 to 624 ± 154 ms, $n = 6$ (Fig. 4C), caused by a slowdown of the diastolic depolarization rate (DDR) from 70 ± 17 to 21 ± 6 mV/s (Fig. 4E). The average maximal diastolic potential (MDP) at the beginning of the pacemaker potential was shifted toward more negative potentials, from −51.7 ± 4.4 to −57.6 ± 6.0 mV (Fig. 4D). This difference, however, was not significant, possibly because of a high variability of this parameter. The action potential duration (i.e., the duration from reaching the threshold potential at approximately −40 mV) to the return of the potential to the MDP was prolonged from 200 ± 16 to 323 ± 33 ms (Fig. 4F). This

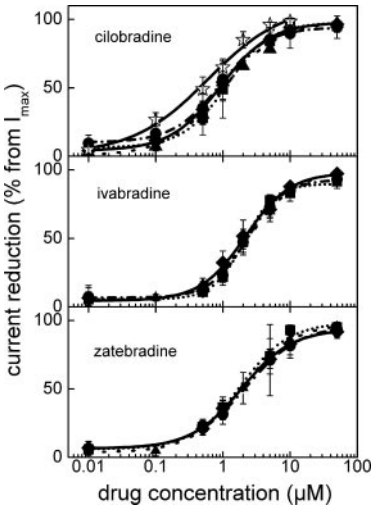

Fig. 3. Steady-state inhibition of HCN1, HCN2, HCN3, and HCN4 channels by cilobradine, ivabradine, and zatebradine and the inhibition of sinoatrial I_f by cilobradine. Values are mean inhibition ± S.D. of currents at the indicated drug concentration determined after 500 activations for HCN1 and HCN2, after 50 activations for HCN3 and HCN4, and after 30 activations for I_f. n numbers used to establish the curves are given in Table 1. Superimposed dose-response curves represent logistic fits of means. The meaning of symbols are the following, for all three: square/short-dotted line, HCN1; circle/broken-dotted line, HCN2; triangle/dotted line, HCN3; diamond/broken line: HCN4; open stars/solid line, I_f.

TABLE 1

Effects of sinus node inhibitors on HCN channels and I_f in sinoatrial node cells and in vivo

IC_{50} values and slopes of logistic fit (Hill coefficient) of the dose-response curves displayed in Fig. 3 for cilobradine, ivabradine, and zatebradine on expressed HCN channels. In addition, the IC_{50} value for cilobradine on native I_f recorded from isolated mouse sinoatrial node cells was determined. ED_{50} values for the three drugs were determined by analyzing the bradycardic effect in mice (Fig. 6A). Numbers in parentheses give the number of mice/cells used to establish the dose-response curves.

HCN Subtype	IC_{50}	Hill Coefficient
	μM	
Cilobradine, 1.2 mg/kg (10 animals)		
HCN1 (33)	1.15 ± 0.16	1.3 ± 0.24
HCN2 (42)	0.90 ± 0.07	1.3 ± 0.13
HCN3 (37)	0.99 ± 0.16	1.1 ± 0.18
HCN4 (37)	0.92 ± 0.05	1.2 ± 0.09
I_f (28)	0.62 ± 0.18	0.8 ± 0.22
Ivabradine, 4.7 mg/kg (6 animals)		
HCN1 (56)	2.05 ± 0.13	1.9 ± 0.19
HCN2 (27)	2.29 ± 0.13	1.6 ± 0.12
HCN3 (38)	2.51 ± 0.13	1.3 ± 0.07
HCN4 (17)	2.15 ± 0.34	1.3 ± 0.22
Zatebradine, 1.8 mg/kg (10 animals)		
HCN1 (27)	1.83 ± 0.39	1.2 ± 0.22
HCN2 (26)	2.21 ± 0.21	1.1 ± 0.08
HCN3 (24)	1.90 ± 0.13	1.1 ± 0.08
HCN4 (22)	1.88 ± 0.12	1.2 ± 0.06

prolongation was caused by a slightly slower repolarization velocity of 0.47 versus 0.62 V/s in the absence of cilobradine (Fig. 4G). The slower repolarization velocity contributed only marginally to the slower AP rate. Because the impairment of repolarization is caused by a block of repolarizing potassium currents and might cause serious rhythm problems such as torsades-de-pointes arrhythmias, we tested the effect of a high dose of cilobradine (5 μM) on the outward potassium currents of myocytes isolated from murine atria (data not shown). In agreement with findings by Goethals et al. (1993), cilobradine induced a small block of the fast-activating phase of repolarizing potassium currents (from 21 $\pm$ 3 to 16.4 $\pm$ 2 pA/pF at 60 mV, $n = 12$ cells). This reduction was significant at $p < 0.05$ and could be responsible for the slightly delayed repolarization. The depolarization (upstroke) velocity, presumably carried by calcium and sodium currents, was not changed significantly by this SNI (0.999 $\pm$ 0.05 versus 0.991 $\pm$ 0.08 V/s; data not shown).

Incubation with high concentrations of cilobradine up to 10 μM did not slow the DDR further. However, the cycle lengths (CL) became increasingly variable. Figure 4H shows that 1 μM cilobradine already increased significantly the S.D. of the CL. This increasing CL-SD corresponds to the increasing heart rate variability in mice as described below.

SNIs Cause Bradycardia and Arrhythmia in Mice. Telemetric ECG recordings in mice allowed the analysis of the heart rate and ECG parameters in response to the application of SNIs in an unrestrained state for the animal. In-

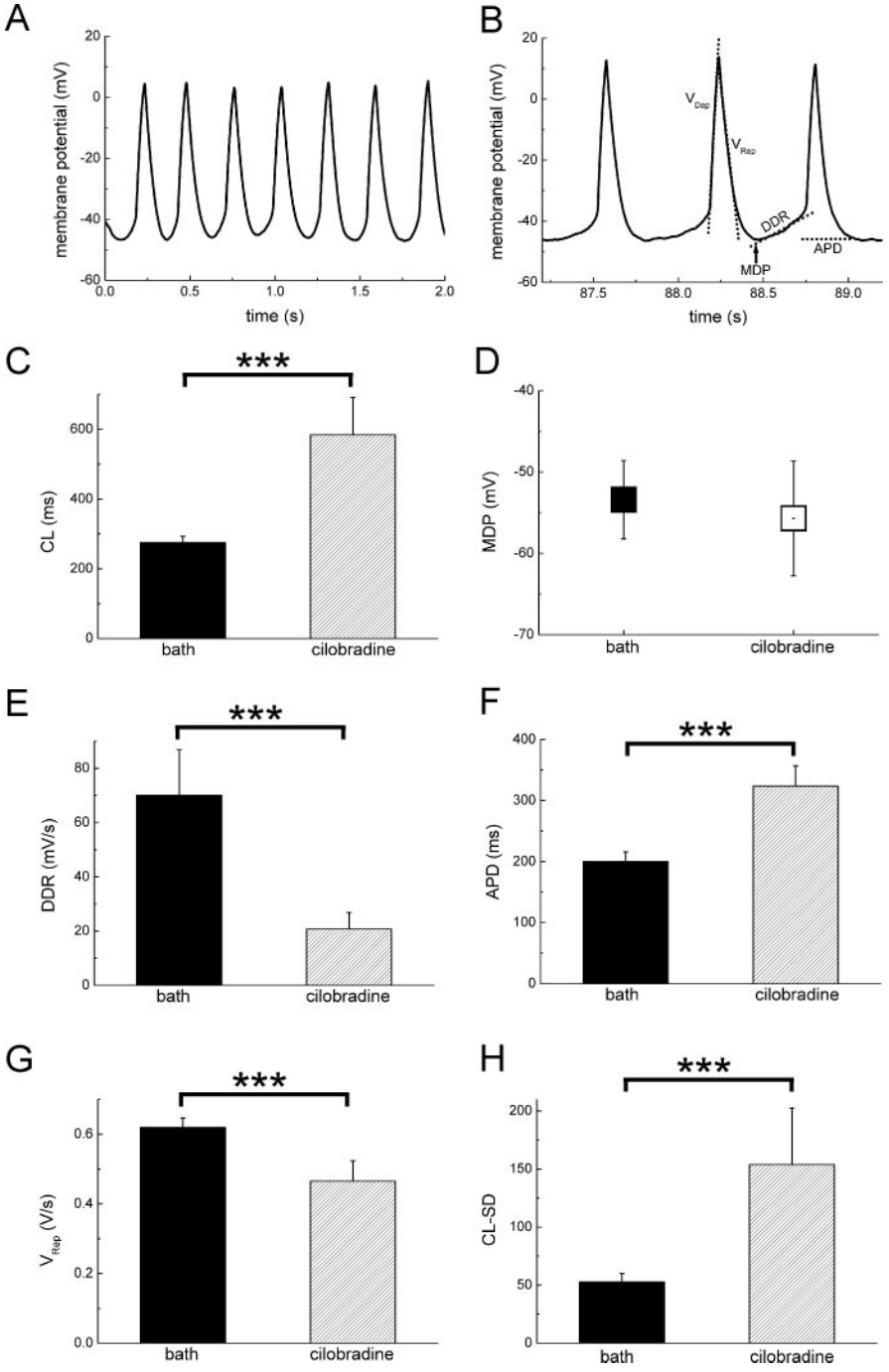

Fig. 4. Effect of 1 μM cilobradine on spontaneous APs recorded from isolated murine sinoatrial node cells at 32°C. Example of APs recorded from the same cell before (A) and 60 s after (B) application of the SNI. Parameters shown in C to H are depicted in B. C to H, comparison of CL (C), MDP (D), DDR (E), action potential duration (APD, F), repolarization velocity (V_{Rep}, G), and CL-SD (H) of APs recorded before ("bath") and after ("cilobradine") drug application. Values are mean $\pm$ S.D., $n = 6$. ***, $p < 0.001$. Of the AP parameters, all except for MDP differ significantly before and after the application of cilobradine. The increase in CL-SD (H) indicates increasing AP arrhythmia in the presence of the SNI.

traperitoneal injection of cilobradine dose-dependently reduced the heart rate and increased its variability (Fig. 5). Identical results were obtained with ivabradine and zatebradine but not with verapamil (Fig. 6A). The reduction of the heart rate started at doses of 0.5 mg/kg. The slowest heart rate that could be reached with the SNIs was approximately 200 bpm. No slower heart rates were reached, even at progressively higher doses. The ED_{50} values for the decrease in heart rate were in a similar range, with cilobradine having the lowest ED_{50} value with 1.2 mg/kg followed by zatebradine (1.8 mg/kg) and ivabradine (4.7 mg/kg) (Table 1). Again, the heart rate was reduced because the R-R interval durations increased in the presence of SNIs (Fig. 6B, top) and so did the variability of the R-R intervals, as demonstrated by the increasing standard deviation of the R-R intervals (Fig. 6B, bottom). Doses greater than 5 mg/kg of the SNIs, however, had an additional effect on the heart rate. They induced a periodic arrhythmia (Fig. 5, bottom). This type of arrhythmia started at approximately 7.5 mg/kg cilobradine, 10 mg/kg zatebradine, and 12.5 mg/kg ivabradine. The arrhythmia consisted of a periodic fluctuation of the R-R interval durations (Fig. 5, right bottom). This periodicity was characterized by cycles in which the P-P intervals got progressively shorter until one whole ECG complex was omitted, and the cycle started again with a longer P-P interval (Fig. 7, A and B). An AV conduction block did not seem to be the cause for the arrhythmia, because the PQ intervals showed no abnormal variations during one cycle of arrhythmia (37.9 ± 5.1 ms), and once a P wave occurred, all following peaks and waves of the ECG complex (Q, R, S, and T) were invariably present.

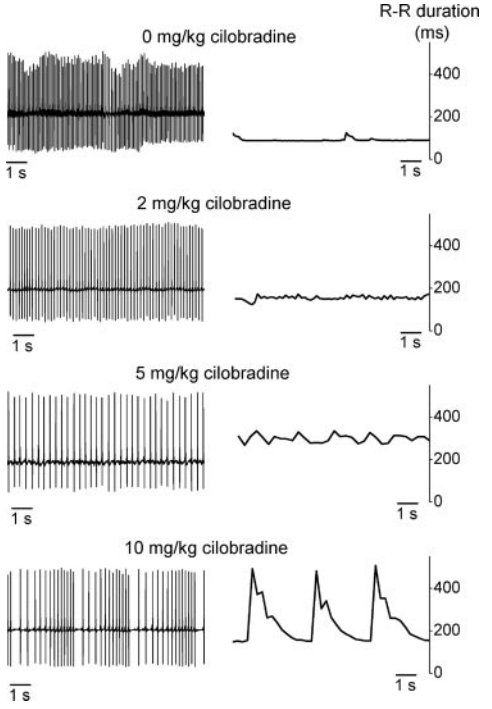

Fig. 5. Examples of telemetric ECG recordings in freely moving mice after injection of an SNI. Left, recordings from a mouse 30 min after intraperitoneal injection with saline or 2, 5, or 10 mg/kg cilobradine. Right, the corresponding R-to-R interval durations obtained by peak-to-peak analysis of the ECG complexes; 2 and 5 mg/kg cilobradine induce increasing bradycardia without abnormal arrhythmia, and 10 mg/kg cilobradine induces bradycardia and arrhythmia characterized by periodic fluctuations of the R-R durations.

The only interval of the ECG complex that was consistently and in parallel with the P-P interval (Fig. 7B) affected by increasing doses of cilobradine was the duration between the end of the T wave and the beginning of the following P wave. This TP interval is basically the diastolic interval and includes the (usually nonvisible) slow spontaneous depolarization of the sinus node that leads to the excitation of the atria, visible as P wave. After injection of saline, 2 mg/kg cilobradine, which induces bradycardia, and 10 mg/kg cilobradine, which induces bradycardia and arrhythmia, the TP duration changed significantly with every dose from a mean of 47 ± 7 (control) to 70 ± 13 ms (2 mg/kg) to 142 ± 38 ms (10 mg/kg) (Fig. 7C). Ivabradine and zatebradine had qualitatively the same effects on the ECG parameters as cilobradine only that higher doses were needed in agreement with their higher ED_{50} values. SNIs also prolonged the net QT duration, an effect caused by their impact on the heart rate. However, the heart rate-corrected QT durations are not prolonged even at high doses of SNIs (Fig. 7C). This result suggested that even though repolarization velocity and repolarizing potassium currents of single cardiac cells are slightly inhibited by a high dose of the drugs (demonstrated for cilobradine, Fig. 4), this

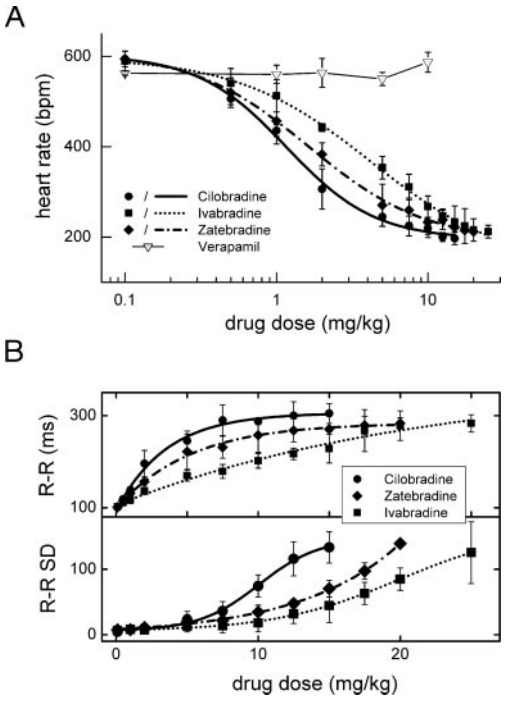

Fig. 6. Dose-dependent heart rate reduction and arrhythmia induction in mice by SNIs. A, heart rates (in beats per minute) 30 min after intraperitoneal injection of cilobradine, ivabradine, and zatebradine at the indicated doses. Symbols represent the mean ± S.D., and superimposed dose-response curves represent the logistic fits of the means. Mean heart rates after injection of verapamil are also given, but no fit was found because verapamil did not affect the heart rate at doses comparable with the SNIs; $n = 6$ to 10 mice per dose and drug (also given in Table 1). The ED_{50} value of ivabradine differs significantly at $p < 0.001$ from both cilobradine and zatebradine. B, R-R intervals (top) and the R-R standard deviation from beat to beat (bottom) as a means to describe arrhythmia after injection of indicated doses of the drugs. All drugs induce arrhythmia at doses greater than 5 mg/kg, with ivabradine requiring the highest and cilobradine the lowest dose for the arrhythmia to appear. Symbols represent the mean ± S.E.M., fits represent exponential fit at the top and sigmoidal fit at the bottom; circles/solid line, cilobradine; diamonds/broken-dotted line, zatebradine; squares/dotted line, ivabradine. Note that for linear scales in B, n numbers are the same as in A.

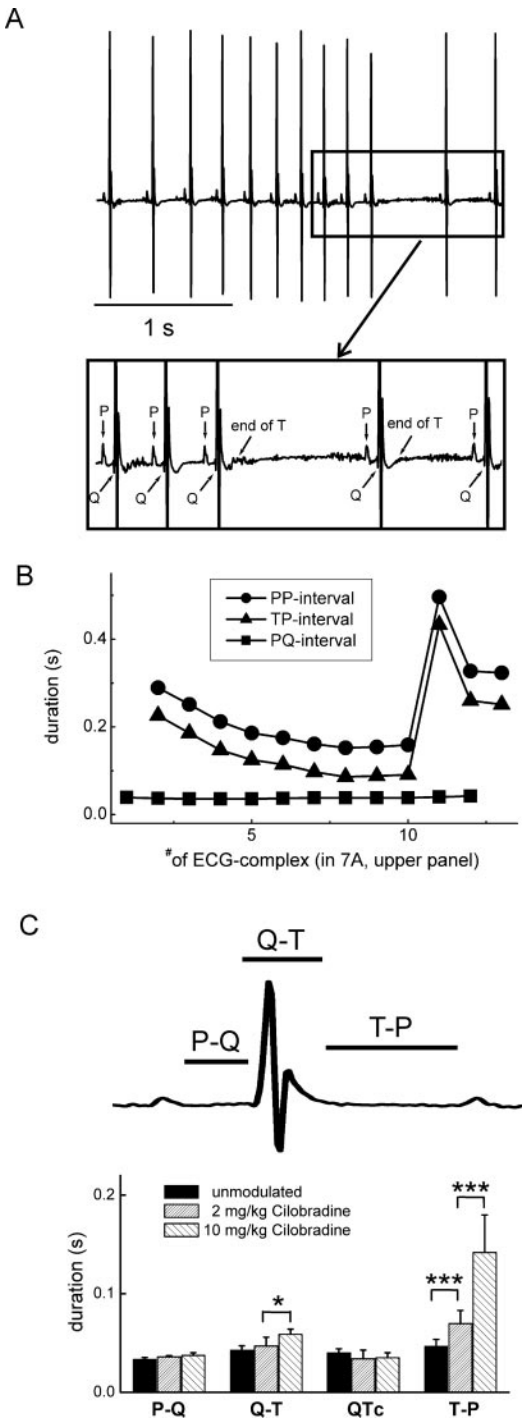

Fig. 7. Effects of SNIs on the cardiac electrical activity in mice. A, enlarged ECG examples from Fig. 5, bottom, showing one cycle of the typical arrhythmia caused by a high dose of the SNI cilobradine. P, Q, and end of T (here: return of negative part of T deviation to isoelectric line), from which the parameters in B were calculated, are indicated in the bottom enlargement. B, P-P, TP, and PQ durations corresponding to the ECG stretch displayed in A, top. The duration of the P-P interval decreases with each heart beat until a pause occurs. This fluctuation in P-P durations is independent of the PQ durations but is caused by equally varying TP durations. C, statistical analysis of the TP-, PQ-, QT-, and QTc durations; $n = 6$ mice, with analysis performed on a 20-s ECG stretch per animal, before ("unmodulated") and after application of 2 or 10 mg/kg drug. The TP duration is highly significantly prolonged by SNIs, and fluctuations in the TP duration are responsible for the arrhythmia. SNIs also prolong the QT duration significantly, but the heart rate-corrected QTc duration is not significantly different. *, $p < 0.05$; ***, $p < 0.001$.

inhibition does not seem to change significantly the repolarization time in the whole animal at reasonable SNI doses.

Impaired Up-Regulation of the Heart Rate after Inhibition of I_f. Binding of cAMP to HCN channels has been implicated to participate in the sympathetic up-regulation of the beating frequency. To explore the role of I_f in heart rate regulation at stress, we performed two sets of experiments in mice: pharmacological stimulation with isoproterenol, and forced physical activity. Injection of 0.5 mg/kg isoproterenol alone increased the heart rate from a mean of 506 ± 85 to 721 ± 20 bpm within 10 min (Fig. 8, A and C). After approximately 1 h, the heart rate returned to a resting value, which was not different from the heart rate after injection of NaCl as a control. Injection of 5 mg/kg cilobradine slowed the heart rate to a mean of 250 ± 42 bpm within 30 min, and this effect lasted for more than 3 h. It is noteworthy that the heart rate after injection of 5 mg/kg cilobradine and, 30 min later, 0.5 mg/kg isoproterenol (Fig. 8A, bottom) still increased, but not above a low resting value of 428 ± 15 bpm. Physical activity, like running on a treadmill, increased the heart rate to 744 ± 25 bpm, similar to an isoproterenol injection (Fig. 8, B and C). However, running after an injection of 5 mg/kg cilobradine increased the heart rate only to 442 ± 25 bpm, not further, again similar to the experiment with the pharmacological stimulation. These results indicated that an up-regulation of the heart rate under the condition of presumably blocked I_f is still possible but is impaired. Because it was possible that the blocked I_f could be simply unblocked by the binding of cAMP, we tested the effect of cilobradine on cloned HCN channels and native I_f in the absence and presence of cAMP (Fig. 8D). Addition of the membrane-permeable cAMP analog on 8-bromoadenosine-cAMP, however, increased neither the steady-state HCN4 current in HEK293 cells nor the sinoatrial I_f after the currents had been blocked by 1 μM cilobradine. These findings suggest that a basic up-regulation of the heart rate is independent of I_f, but faster heart rates require I_f.

Discussion

The results of this study can be summarized as follows: 1) Cilobradine, ivabradine, and zatebradine block all four HCN channels with the same IC_{50} value and provide no subtype-specific blocker. As reported previously for native I_f (Bogaert et al., 1990; Bucchi et al., 2002), the block is use-dependent. The use-dependence is affected by the subtype of the channel; 2) cardiac rhythm in mice is decreased to a basal frequency and can not be further lowered even by supramaximal doses of SNIs; 3) high doses of SNIs induce periodic arrhythmia that has the characteristics of a second-degree sinoatrial block; and 4) the sympathetic stimulation of the heart rate remains possible but is impaired in the presence of an apparent complete block of I_f by high doses of SNIs.

These findings are in line with previous reports (Schram et al., 2002; Satoh, 2003; Mangoni et al., 2005) that regulation of the heart rate depends on several independent mechanisms. Our experiments showed that both the normal heart rate and up-regulation of the heart rate higher than resting values require an intact I_f. A characteristic feature of I_f and HCN channels is their direct modulation by cAMP (Robinson and Siegelbaum, 2003; Baruscotti et al., 2005). Binding of cAMP to HCN4 shifts the voltage dependence of channel opening to more positive values and increases thereby the

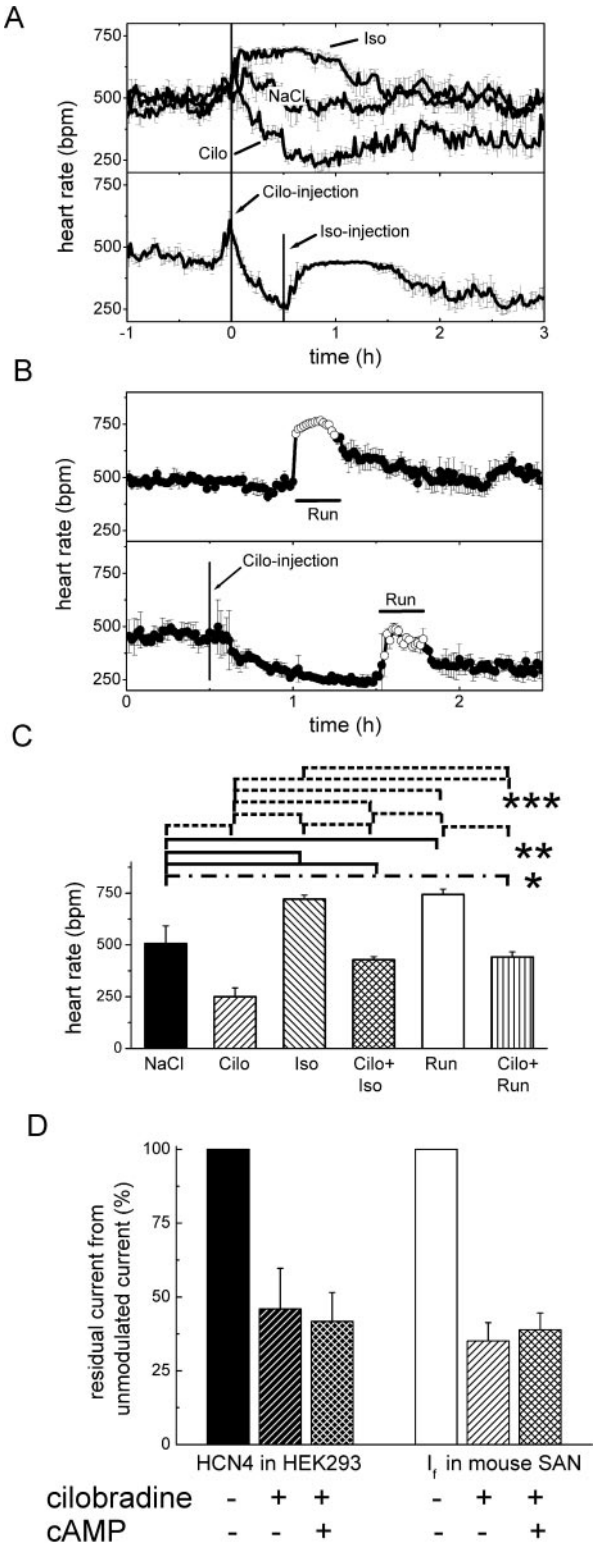

Fig. 8. Reduced sympathetic up-regulation of the heart rate in mice after application of an SNI. A, time course of heart rate after intraperitoneal injection of cilobradine and isoproterenol (β-adrenergic stimulation). A, top, heart rate after the injection of 100 μl of 0.9% NaCl as control (NaCl, broken line), 5 mg/kg cilobradine (Cilo, solid line), or 0.5 mg/kg isoproterenol (Iso, broken-dotted line). Injection was done at time point 0 (vertical line). A, bottom, heart rate after cilobradine/isoproterenol injection; 5 mg/kg cilobradine was injected at $t = 0$ (first vertical line), and 0.5 mg/kg isoproterenol was injected 30 min after cilobradine (second vertical line). The β-adrenergic stimulation was only able to increase the heart rate from bradycardia (approximately 250 bpm) to a low-resting level of approximately 450 bpm, compared with up to 750 bpm after the injection of isoproterenol without cilobradine; $n = 6$ mice for each experiment, and each experiment was done twice. Values are mean ± S.D. B, heart rate before, during, and after a 10-min run on a treadmill. B, without (top) and with (bottom) injection of 5 mg/kg cilobradine before the run. Similar to the drug-induced β-adrenergic stimulation, the SNI prevents up-regulation of the heart rate above a low-resting level. C, statistical analysis of the heart rate modulations shown in A and B. For this analysis, the heart rate reached 30 min after the injection at $t = 0$ (A, top) or after the second injection (A, bottom) or the maximum reached during the run (B) was taken. Levels of significance are indicated. Broken-dotted lines/*, $p < 0.05$; Solid lines/**, $p < 0.01$; broken lines/***, $p < 0.001$. D, HCN currents or I_f, blocked by cilobradine, cannot be "unblocked" by cAMP. Partial block of HCN4 channels (left) or I_f (right) by 1 μM cilobradine was obtained by repeated activation steps to −100 mV as described in Fig. 2 and is given as residual current from unmodulated currents, which are set to 100%. In the presence of 1 μM cilobradine, 100 μM 8-bromoadenosine-cAMP was then added to the bath solution, whereas inward currents were continuously elicited by steps to −100 mV.

DDR in vivo. However, the persistence of a basic heart rate even when I_f is maximally blocked suggests that I_f is not responsible for the basic pacemaker action potential, supporting notions of other mechanisms for the generation of a slow spontaneous diastolic depolarization independent of I_f, which include the activation of several depolarizing currents ($I_{Ca,T}$, $I_{Ca,L}$, I_{st}, $I_{Na/Ca}$, and calcium release from SR) and the inactivation of hyperpolarizing potassium currents. We cannot absolutely rule out that even in the presence of high doses of SNIs, some depolarizing current through HCN channels still flows, because there is always an equilibrium between blocked and unblocked channels. In contrast to this consideration, an up-regulation of the heart rate in the presence of SNIs was only possible from approximately 200 to 450 bpm, not further. This basic up-regulation upon sympathetic stimulation is most likely caused by a mechanism that does not involve I_f but rather modulation of I_{st} (Mitsuiye et al., 2000), I_{Ca} currents, and/or Ca^{2+} release through ryanodine receptors (Satoh, 2003; Mangoni et al., 2005).

The relation of blocked I_f in the cardiac conduction system and bradycardia has been established and needs no further consideration (DiFrancesco and Camm, 2004; Baruscotti et al., 2005). However, the induction of very striking dysrhythmias by each tested SNI has not been described before. Although the sinus node inhibitors have been studied both in vivo (Borer et al., 2003; Vilaine et al., 2003; Colin et al., 2004; DiFrancesco and Camm, 2004; Du et al., 2004; Monnet et al., 2004) and in vitro (Goethals et al., 1993; Bogaert and Pittoors, 2003; DiFrancesco and Camm, 2004), reports of a changed variability of heart rates, AP cycle lengths, or diastolic depolarization rates are missing. This lack of information is probably due to the fact that in these previous studies, the drugs had been applied in a dosage and manner to study only the bradycardic effect of the compounds. In addition, many of the in vitro experiments were conducted on Purkinje fibers using electrically triggered action potentials (Bogaert and Pittoors, 2003), which, of course, disguises any spontaneous arrhythmia. We found similar arrhythmias both in the living mouse and, using the most efficient HCN blocker cilobradine, in isolated sinoatrial node cells, pointing to the conclusion that in the whole animal, the observed arrhythmia, like the bradycardia, originated in the "leading" pacemaker cell.

Periodic arrhythmias are often associated with Wenckebach's periodicity. Normal Wenckebach's periodicity is typ-

ical for a second-degree atrioventricular conduction block. In this condition, the AV conduction is impaired, leading to an elongation of the PQ interval from beat to beat until the interval becomes too long for conduction through the AV node to occur, resulting in one omitted QRS complex after a P wave. After that, a new Wenckebach's cycle with a normal PQ interval starts. In our study, the animals did not show any AV conduction delay. The PQ intervals did not show unusual variations from beat to beat, and isolated P waves without a following QRS complex did not occur. Rather, during one cycle of arrhythmia, the R-R intervals became progressively shorter until one whole ECG complex was left out. This is a sign for a second-degree sinoatrial block, sometimes called "sinoatrial-Wenckebach's" periodicity. In accordance with this, the only ECG interval that was affected by SNIs was the TP duration, which represents the diastolic phase in which the sinoatrial excitation builds up, eventually leading to the excitation of the atria, visible as the P wave.

With the data available to date, we propose two basic mechanisms that, probably in combination, could underlie this periodic disturbance of sinus node excitation after the application of SNIs. First, inhibition of I_f has different effects on individual sinoatrial node cells because the sinus node is a heterogeneous structure. The cells in the center are postulated to function as leading pacemaker cells. Ion-channel density, including I_f, increases from center to periphery (Kodama et al., 2004) and so does conduction velocity. The AP rate in the intact sinus node is highest in the center, complying with the function as leading pacemaking site, but, paradoxically, in isolated cells from the sinus node, the AP rate is higher in cells from the periphery. SNIs could have a stronger impact on the leading pacemaker cells with their smaller current density. Sooner or later, they fire too slowly, so cells from the periphery initiate the next beat. Without the depolarizations and regulations from the center, their firing rate gets faster and faster, until nonpacemaking atrial cells interfere or excitation-refractory is reached, causing the pause. Then, a slower pacemaker cell in the center can take over again. Second, the arrhythmia could arise in one leading pacemaker cell because SNIs have been shown to block I_k and $I_{Ca,L}$ (but not $I_{Ca,T}$) at high concentrations in addition to I_f in SAN cells (Goethals et al., 1993; DiFrancesco and Camm, 2004). The block of these currents was not very effective: 10 μM zatebradine or ivabradine blocked I_K by 18 and 16%, respectively, and $I_{Ca,L}$ by 7% and 18%, respectively. Still, this could lead to an imbalance of the ionic mechanisms usually working together in pacemaking: The block of depolarizing currents (I_f and $I_{Ca,L}$) in sinoatrial node cells, or of the repolarizing I_K in the myocardium, would result in a slower AP rate, but the block of the outward I_K in sinoatrial node cells, on the other hand, would tend to accelerate the diastolic depolarization by keeping the membrane potential closer to the AP threshold potential. Depending on the degree of block of the individual currents, this results only in bradycardia or additional arrhythmia.

Because a large I_f is present in other parts of the cardiac conduction system as well, the question might arise of why the inhibition of this current does not influence conduction. I_f probably has no influence on triggered action potentials. Although Purkinje fibers have a certain potential for spontaneous depolarizations, this activity is normally overridden by the oncoming depolarizations from faster firing cells. On the other hand, the inhibition of I_f in the whole cardiac conduction system may be the reason for the lack of escape rhythms, even though no excitation of the sinus node was sometimes observed for several seconds (corresponding to up to 40 heart beats in the mouse) during the arrhythmias.

We did find slight subtype-specific differences in the use-dependent onset of the block, even when, in the case of HCN2 and HCN3, the same activation/deactivation times and thus exposure times to the drugs were used. This is in accordance with available data from other groups. The block of I_f by cilobradine in sheep Purkinje fibers (Bogaert and Pittoors, 2003) or mouse sinoatrial node cells in our experiments or by ivabradine in rabbit sinoatrial node cells (Bucchi et al., 2002) was completed after 40 activations, whereas 150 to 200 activations were required to block the I_h recorded from mouse dorsal root ganglion neurons (Raes et al., 1998). Assuming HCN4 to be the major HCN subtype of I_f in the cardiac conduction system and HCN1 and HCN2 to be the major neuronal subtypes, the data match, even though the molecular basis for this remains to be documented.

To study the effect of I_f inhibition in vivo, the time to onset of action might be less important than the steady-state inhibition. There were no differences in the steady-state inhibition between the HCN subtypes, although the three used SNIs differed slightly in their IC_{50} values. Cilobradine was the most effective HCN current blocker, followed by zatebradine and ivabradine. This order of efficiency is very interesting because it is exactly the order determined for both the induction of bradycardia and arrhythmia in vivo. This similarity suggests that both conditions are primarily caused by an increasing block of HCN channels despite the potential involvement of other ionic mechanism discussed above.

In conclusion, SNIs cause bradycardia and arrhythmia primarily by inhibition of I_f, which impairs the slow diastolic depolarization of sinoatrial pacemaker cells. The major physiological role of I_f seems to be its contribution to the pacemaker potential at fast heart rates.

Acknowledgments

We thank Natalie Krahmer and Evi Kiermayer for some excellent electrophysiological recordings. Technical assistance from Anna Thomer is highly appreciated.

References

Baruscotti M, Bucchi A, and DiFrancesco F (2005) Physiology and pharmacology of the cardiac pacemaker ("funny") current. *Pharmacol Ther* **107:**59–79.
Bogaert PP, Goethals M, and Simoens C (1990) Use- and frequency-dependent blockade by UL-FS 49 of the I_f pacemaker current in sheep cardiac Purkinje fibres. *Eur J Pharmacol* **187:**241–256.
Bogaert PP and Pittoors F (2003) Use-dependent blockade of cardiac pacemaker current (I_f) by cilobradine and zatebradine. *Eur J Pharmacol* **478:**161–171.
Bois P, Bescond J, Renaudon B, and Lenfant J (1996) Mode of action of bradycardic agent, S 16257, on ionic currents of rabbit sinoatrial node cells. *Br J Pharmacol* **118:**1051–1057.
Borer JS, Fox K, Jaillon P, and Lerebours G (2003) Antiangial and antiischemic effects of ivabradine, an I_f inhibitor, in stable angina. *Circulation* **107:**817–823.
BoSmith RE, Briggs I, and Sturgess NC (1993) Inhibitory actions of ZENECA ZD7288 on whole-cell hyperpolarization activated inward current (I_f) in guinea-pig dissociated sinoatrial node cells. *Br J Pharmacol* **110:**343–349.
Bucchi A, Baruscotti M, and DiFrancesco D (2002) Current-dependent block of rabbit sino-atrial node I_f channels by Ivabradine. *J Gen Physiol* **120:**1–13.
Colin P, Ghaleb B, Monnet X, Hittinger L, and Berdeaux A (2004) Effect of graded heart rate reduction with ivabradine on myocardial oxygen consumption and diastolic time in exercising dogs. *J Pharmacol Exp Ther* **308:**236–240.
DiFrancesco D and Camm JA (2004) Heart rate lowering by specific and selective I_f current inhibition with ivabradine. *Drugs* **64:**1757–1765.
Du XJ, Feng X, Gao XM, Tan TP, Kiriazis H, and Dart AM (2004) I_f channel inhibitor ivabradine lowers heart rate in mice with enhanced sympathoadrenergic activities. *Br J Pharmacol* **142:**107–112.
Goethals M, Raes A, and Bogaert PP (1993) Use-dependent block of the pacemaker

current I_f in rabbit sinoatrial node cells by Zatebradine (UL-FS 49). *Circulation* **88:**2389–2401.
Kodama I, Honjo H, Dobrzynski H, and Boyett M (2004) Cellular mechanisms of sinoatrial activity, in *Cardiac Electrophysiology. From Cell to Bedside* (Zipes DP and Jalife J eds) pp 192–202, Saunders/Elsevier Inc., Philadelphia.
Ludwig A, Budde T, Stieber J, Moosmang S, Wahl C, Holthoff K, Langebartels A, Wotjak C, Munsch T, Zong XG, et al. (2003) Absence epilepsy and sinus dysrhythmia in mice lacking the pacemaker channel HCN2. *EMBO (Eur Mol Biol Organ) J* **22:**216–224.
Ludwig A, Zong X, Stieber J, Hullin R, Hofmann F, and Biel M (1999) Two pacemaker channels from human heart with profoundly different activation kinetics. *EMBO (Eur Mol Biol Organ) J* **18:**2323–2329.
Ludwig A, Zong XG, Jeglitsch M, Hofmann F, and Biel M (1998) A family of hyperpolarization-activated mammalian cation channels. *Nature (Lond)* **393:**587–591.
Mangoni ME, Couette B, Marger L, Bourinet E, Striessnig J, and Nargeot J (2005) Voltage-dependent calcium channels and cardiac pacemaker activity: from ionic currents to genes. *Prog Biophys Mol Biol* **90:**38–63.
Mangoni ME and Nargeot N (2001) Properties of the hyperpolarization-activated current (I_f) in isolated mouse sino-atrial cells. *Cardiovasc Res* **52:**51–64.
Marionneau C, Couette B, Liu J, Li H, Mangoni ME, Nargeot J, Lei M, Escande D, and Demolombe S (2005) Specific pattern of ionic channel gene expression associated with pacemaker activity in the mouse heart. *J Physiol (Lond)* **562:**223–234.
Mitchell GF, Jeron A, and Koren G (1998) Measurement of heart rate and Q-T interval in the conscious mouse. *Am J Physiol* **274:**H747–H751.
Mitsuiye T, Shinagawa Y, and Noma A (2000) Sustained inward current during pacemaker depolarization in mammalian sinoatrial node cells. *Circ Res* **87:**88–91.
Monnet X, Colin P, Ghaleh B, Hittinger L, Giudecelli J-F, and Berdeaux A (2004) Heart rate reduction during exercise-induced myocardial ischaemia and stunning. *Eur Heart J* **25:**579–586.
Raes A, Van de Vijver G, Goethals M, and Bogaert PP (1998) Use-dependent block of I_h in mouse dorsal root ganglion neurons by sinus node inhibitors. *Br J Pharmacol* **125:**741–750.
Robinson RB and Siegelbaum SA (2003) Hyperpolarization-activated cation currents: From molecules to physiological function. *Annu Rev Physiol* **65:**453–480.
Santoro B, Liu D, Yao H, Bartsch D, Kandel ER, Siegelbaum SA, and Tibbs GR (1998) Identification of a gene encoding a hyperpolarization-activated pacemaker channel of brain. *Cell* **93:**717–729.
Satoh H (2003) Sino-atrial nodal cells of mammalian hearts: Ionic currents and gene expression of pacemaker ionic channels. *J Smooth Muscle Res* **39:**175–193.
Schram G, Pourrier M, Melnyk P, and Nattel S (2002) Differential distribution of cardiac ion channel expression as a basis for regional specialization in electrical function. *Circ Res* **90:**939–950.
Stieber J, Herrmann S, Feil S, Löster J, Feil R, Biel M, Hofmann F, and Ludwig A (2003a) The hyperpolarization-activated channel HCN4 is required for the generation of pacemaker action potentials in the embryonic heart. *Proc Natl Acad Sci USA* **100:**15235–15240.
Stieber J, Stöckl G, Herrmann S, Hassfurth B, and Hofmann F (2005) Functional expression of the human HCN3 channel. *J Biol Chem* **280:**34635–34643.
Stieber J, Thomer A, Much B, Schneider A, Biel M, and Hofmann F (2003b) Molecular basis for the different activation kinetics of the pacemaker channels HCN2 and HCN4. *J Biol Chem* **278:**33672–33680.
Vilaine JP, Bidouard JP, Lesage L, Reure H, and Peglion JL (2003) Anti-ischemic effects of ivabradine, a selective heart rate-reducing agent, in exercise-induced myocardial ischemia in pigs. *J Cardiovasc Pharmacol* **42:**688–696.

Address correspondence to: Dr. Juliane Stieber, Institut für Pharmakologie und Toxikologie, TU München, Biedersteiner Str. 29, 80802 München, Germany. E-mail: stieber@ipt.med.tu-muenchen.de